

Supporting Information for “MAP: an MP2 accuracy predictor for weak interactions from adiabatic connection theory”

Stefan Vuckovic,¹ Eduardo Fabiano,² Paola Gori-Giorgi,³ and Kieron Burke¹

¹*Department of Chemistry, University of California, Irvine, CA 92697, USA^a*

²*Institute for Microelectronics and Microsystems (CNR-IMM), Via Monteroni, Campus Unisalento, 73100 Lecce, Italy*

³*Department of Theoretical Chemistry and Amsterdam Center for Multiscale Modeling, FEW, Vrije Universiteit, De Boelelaan 1083, 1081HV Amsterdam, The Netherlands*

S1. Ψ_λ^{HF} WAVE FUNCTION FOR TWO-ELECTRON CLOSED SHELL SYSTEMS

Here we detail the construction of the the Ψ_λ^{HF} wave function, used in Figures 1-3. We remember that Ψ_λ^{HF} minimizes the following Hamiltonian:

$$\hat{H}_\lambda^{\text{HF}} = \hat{T} + \hat{V}_{\text{ext}} + \lambda \hat{V}_{ee} + (1 - \lambda) (\hat{J} + \hat{K}). \quad (\text{S1})$$

To obtain this wave function, we first perform the HF calculation to obtain the set of HF (MO) orbitals: $\phi_1, \phi_2, \phi_3, \dots, \phi_K$. Then we construct spin adapted determinants in terms of these orbitals for two-electron closed shell systems :

$$\Phi_{ij} = \frac{1}{\sqrt{2}} \begin{vmatrix} \phi_i(\mathbf{r}_1)\alpha(\sigma_1) & \phi_j(\mathbf{r}_1)\beta(\sigma_1) \\ \phi_i(\mathbf{r}_2)\alpha(\sigma_2) & \phi_j(\mathbf{r}_2)\beta(\sigma_2) \end{vmatrix} \quad (\text{S2})$$

We can write Ψ_λ^{HF} as a linear combination of Φ_{ij} determinants:

$$\Psi_\lambda^{\text{HF}} = \sum_{i,j} c_{ij}^\lambda \Phi_{ij}. \quad (\text{S3})$$

Then performing a full-CI calculation we can obtain the c_{ij}^λ coefficients.

As usually, the HF orbitals are given in terms of (real) atomic basis functions and the corresponding coefficients :

$$\phi_i = \sum_{r=1}^K c_{ri}^{\text{HF}} \chi_r. \quad (\text{S4})$$

Ingredients that we use for obtaining the c_{ij}^λ coefficients are the bare hamiltonian matrix and a set of two-electron integrals (both of which are in the AO basis), and the c_{ri}^{HF} coefficients. The bare hamiltonian matrix in AO basis is given by:

$$h_{pq}^{\text{AO}} = \langle \chi_p | \hat{T} + \hat{V}_{\text{ext}} | \chi_q \rangle, \quad (\text{S5})$$

and we use the following notation for two-electron integrals in AO basis:

$$(pq|rs) = \int \chi_p(\mathbf{r}_1) \chi_q(\mathbf{r}_1) r_{12}^{-1} \chi_r(\mathbf{r}_2) \chi_s(\mathbf{r}_2) d\mathbf{r}_1 d\mathbf{r}_2. \quad (\text{S6})$$

^a) Electronic mail: svuckovi@uci.edu

Combing eqs S4 and S5, we obtain the bare Hamiltonian matrix in MO basis:

$$h_{ij} = \sum_{p,q} c_{pi}^{\text{HF}} c_{qj}^{\text{HF}} h_{pq}^{\text{AO}}. \quad (\text{S7})$$

Combining eqs S4 and S6, we obtain two-electron integrals in MO basis:

$$U_{ijkl} = \sum_{p,q,r,s} c_{pi}^{\text{HF}} c_{qj}^{\text{HF}} c_{rk}^{\text{HF}} c_{sl}^{\text{HF}} (pq|rs). \quad (\text{S8})$$

To obtain the c_{ij}^λ of eq S3 by the CI calculation we need to construct the $\langle \Phi_{ij} | H_\lambda^{\text{HF}} | \Phi_{kl} \rangle$ matrix elements, where Φ_{ij} is given by eq. S2. The integrals that we need for the construction of $\langle \Phi_{ij} | \hat{H}_\lambda^{\text{HF}} | \Phi_{kl} \rangle$ [see eq S1] are:

$$\langle \Phi_{ij} | \hat{T} + \hat{V}_{\text{ext}} | \Phi_{kl} \rangle = h_{jl} \delta_{ik} + h_{ik} \delta_{jl}, \quad (\text{S9})$$

$$\langle \Phi_{ij} | \hat{V}_{ee} | \Phi_{kl} \rangle = U_{jl ik}, \quad (\text{S10})$$

and

$$\begin{aligned} \langle \Phi_{ij} | \hat{V}_{\text{HF}} | \Phi_{kl} \rangle &= 2(U_{lj11} \delta_{ik} + U_{ik11} \delta_{lj}) \\ &\quad - \frac{1}{2} U_{1j1l} \delta_{ik} - \frac{1}{2} U_{1i1k} \delta_{lj}. \end{aligned} \quad (\text{S11})$$

In eq S11, the first two terms arise from the \hat{J} operator and the last two terms arise from the \hat{K} operator. With matrix elements given in eqs S9, S10 and S11 we can find the c_{ij}^λ coefficients that correspond to the smallest eigenvalue of a matrix pertinent to the Hamiltonian of eq S1.

S2. FITTING FUNCTIONS FOR DFT AC CURVES

In Figure 3 of the manuscript, the second derivative of $W_{c,\lambda}^{\text{HF}}$ for He and H^- has been obtained numerically by a finite difference. While this numerical procedure was very stable when applied to $W_{c,\lambda}^{\text{HF}}$, the second derivative of $W_{c,\lambda}^{\text{DFT}}$ computed this way contained *unphysical* oscillations. To avoid this problem, we use the highly accurate data (FCI/aug-cc-CVTZ) along the DFT AC to fit $W_{c,\lambda}^{\text{DFT}}$ for He and H^- to an analytical function, whose second derivative has been shown in Figure 3 of the manuscript.

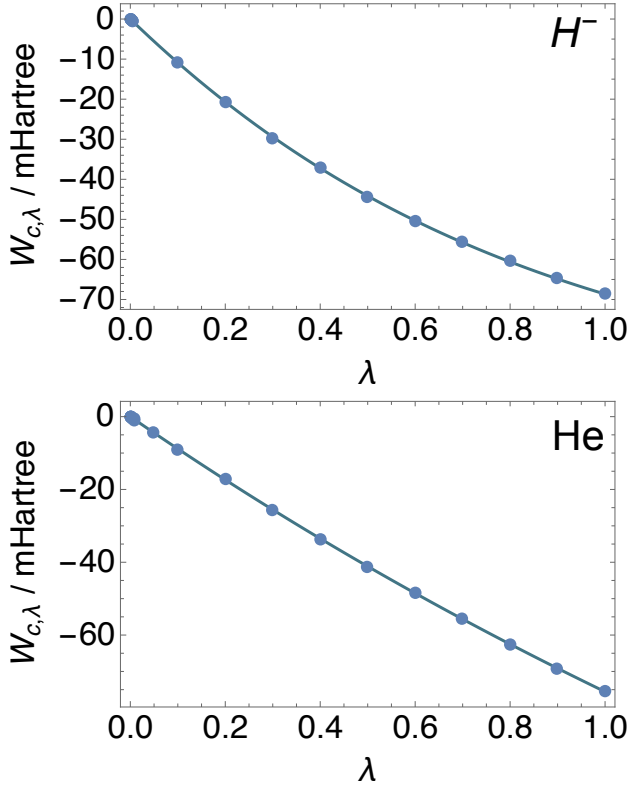


FIG. S1: The DFT AC numerical datapoints (blue dots) for H^- (top panel) and He (bottom panel) and plots showing the fitting function of eq S12

TABLE S1: The parameters for the fitting function of eq S12 for H^- and He

| param. | H^- | He |
|----------------|-----------|-----------|
| E_c^{GL2} | -0.057131 | -0.044995 |
| $W_{c,\infty}$ | -0.185982 | -0.473271 |
| b_3 | 1.0304 | 0.131994 |
| c_1 | 0.487658 | 0.50204 |
| c_2 | 0.463272 | 0.370716 |
| c_3 | 0.345689 | 0.108957 |

For this purpose, we use the following analytical function (akin to an interpolation form proposed in ref 1):

$$W_{c,\lambda} = a + b_1 y_1 + b_2 y_2^4 + b_3 y_3^6, \quad (S12)$$

where

$$y_i = \frac{1}{\sqrt{1 + c_i \lambda}}. \quad (S13)$$

We fix the a , b_1 and b_2 parameters by ensuring that $W_{c,\lambda}$ of Eq S12 satisfies the following constraints:

$$W_{c,0} = 0 \quad (S14)$$

$$\frac{\partial W_{c,0}}{\partial \lambda} = 2E_c^{GL2} \quad (S15)$$

$$\lim_{\lambda \rightarrow \infty} W_{c,\lambda} = W_{c,\infty} = W_{c,\infty}^{SCE}, \quad (S16)$$

where $W_{c,\lambda}^{SCE}$ is the exact value for $W_{c,\infty}$ obtained from the strictly correlated electrons approach². In this way, the fit also contains the accurate information from $\lambda \gg 1$. This sets:

$$a = W_{c,\infty} \quad (S17)$$

$$b1 = \frac{4b_3c_2 - 6b_3c_3 - 4E_c^{GL2} + 4c_2W_{c,\infty}}{c1 - 4c_2}. \quad (S18)$$

The remaining parameters (b_3 , c_1 , c_2 , c_3) have been fitted to the highly accurate data for the λ values between 0 and 1 and the local initial curvature. All highly accurate quantities are taken from Refs. 3 and 4, and, as said, they had been obtained at the full-CI/aug-cc-pCVTZ level. The fitting parameters for He and H^- are given in Table S1. The highly accurate datapoints and the fitted function of eq S12 are also shown in in Fig. S1. By giving errors of less than 0.62% for H^- and less than 0.007% for He, both of the fits are rather accurate.

S3. SIZE-CONSISTENCY CORRECTED AC CURVES MODELS

The size-consistency of adiabatic connection models (ACMs) that depend non-linearly on the ingredients, as the SPL model used here, has been thoroughly discussed in ref 5. Given an interpolation form for $W_{c,\lambda}^{ACM,int}$, the interaction AC is given by the following difference:

$$W_{c,\lambda}^{ACM,int}(M) = W_{c,\lambda}^{ACM}(\mathbf{W}(M)) - \sum_i^N W_{c,\lambda}^{ACM}(\mathbf{W}(F_i)). \quad (S19)$$

Applying the size-consistency correction (SCC) correction introduced in ref 5 (see this ref for further details), $W_{c,\lambda}^{ACM,int}(M)$ would read as:

$$W_{c,\lambda}^{ACM,int}(M) = W_{c,\lambda}^{ACM}(\mathbf{W}(M)) - W_{c,\lambda}^{ACM} \left(\sum_i^N \mathbf{W}(F_i) \right). \quad (S20)$$

In Figure S2, we show the interpolated AC curves obtained from different interpolation forms. These include the SPL form together with other forms proposed in the literature [see ref 5 for the full mathematical details of the forms]. In this figure we show the interpolated AC curves when the SCC is turned on (i.e. those computed from eq S20) represented by solid lines) and interpolated AC curves without the SCC (i.e. those computed from eq S19). We can see from Figure S2, that the $W_{c,\lambda}^{ACM,int}$ curves obtained without the SCC look very different. We can also see that when the SCC is turned on, they look very similar. We can also see from the table shown in the inset of figure S2 that the AC curves with SCC give rise to even by an order of magnitude more accurate interaction energies than those curves without SCC. This observation is in line with ref 5, where it has been shown that the SCC can drastically improve the accuracy of

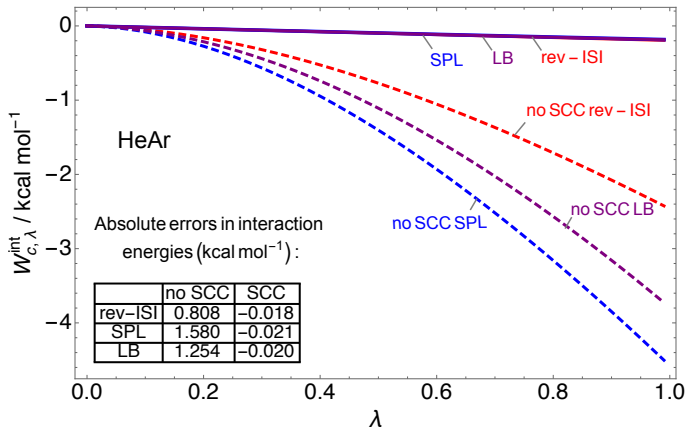


FIG. S2: Interaction energies AC curves obtained with the rev-ISI, SPL and LB functionals with (eq S20) and without the SCC (eq S19) for the HeNe and HeAr dimers. The table in the insets shows absolute energies for the total interaction energies

the ACM models. For this reason, in this paper we always apply the SCC when we compute $W_{c,\lambda}^{\text{ACM,int}}(M)$ (via eq S20) and the corresponding λ_{ext} values.

S4. MAP VALUES FOR THE S22 DATASET

TABLE S2: MAP values for the S22 dataset

| num. | system | MAP |
|------|------------------------------|-------|
| 1 | (NH3)2 | 0.140 |
| 2 | (H2O)2 | 0.072 |
| 3 | Formic acid dimer | 0.023 |
| 4 | Formamide dimer | 0.086 |
| 5 | Uracil Dimer | 0.097 |
| 6 | 2-pyridoxine-2-aminopyridine | 0.171 |
| 7 | Adenine-thymine WC | 0.159 |
| 8 | (CH4)2 | 0.134 |
| 9 | (C2H4)2 | 0.173 |
| 10 | Benzene-CH4 | 0.198 |
| 11 | PD Benzene Dimer | 0.232 |
| 12 | Pyrazine dimer | 0.229 |
| 13 | Uracil dimer | 0.209 |
| 14 | Stacked indole-benzene | 0.235 |
| 15 | Stacked adenine-thymine | 0.222 |
| 16 | Ethene-ethyne | 0.148 |
| 17 | Benzene-H2O | 0.172 |
| 18 | Benzene-NH3 | 0.191 |
| 19 | Benzene-HCN | 0.173 |
| 20 | T-shaped benzene dimer | 0.214 |
| 21 | T-shaped indole benzene | 0.216 |
| 22 | Phenol dimer | 0.195 |

S5. MAP VALUES FOR THE S66 DATASET

TABLE S3: MAP values for the S66 dataset. Complexes 1-23: 'hydrogen bonds', complexes 24-46: 'dispersion', complexes 47-66: 'others'

| num. | system | MAP |
|------|-------------------------------|-------|
| 1 | Water ... Water | 0.066 |
| 2 | Water ... MeOH | 0.113 |
| 3 | Water ... MeNH2 | 0.137 |
| 4 | Water ... Peptide | 0.090 |
| 5 | MeOH ... MeOH | 0.132 |
| 6 | MeOH ... MeNH2 | 0.159 |
| 7 | MeOH ... Peptide | 0.126 |
| 8 | MeOH ... Water | 0.094 |
| 9 | MeNH2 ... MeOH | 0.152 |
| 10 | MeNH2 ... MeNH2 | 0.175 |
| 11 | MeNH2 ... Peptide | 0.172 |
| 12 | MeNH2 ... Water | 0.147 |
| 13 | Peptide ... MeOH | 0.158 |
| 14 | Peptide ... MeNH2 | 0.177 |
| 15 | Peptide ... Peptide | 0.161 |
| 16 | Peptide ... Water | 0.113 |
| 17 | Uracil ... Uracil (BP) | 0.114 |
| 18 | Water ... Pyridine | 0.148 |
| 19 | MeOH ... Pyridine | 0.169 |
| 20 | AcOH ... AcOH | 0.040 |
| 21 | AcNH2 ... AcNH2 | 0.099 |
| 22 | AcOH ... Uracil | 0.070 |
| 23 | AcNH2 ... Uracil | 0.086 |
| 24 | Benzene ... Benzene (pi-pi) | 0.231 |
| 25 | Pyridine ... Pyridine (pi-pi) | 0.229 |
| 26 | Uracil ... Uracil (pi-pi) | 0.209 |
| 27 | Benzene ... Pyridine (pi-pi) | 0.230 |
| 28 | Benzene ... Uracil (pi-pi) | 0.221 |
| 29 | Pyridine ... Uracil (pi-pi) | 0.219 |
| 30 | Benzene ... Ethene | 0.221 |
| 31 | Uracil ... Ethene | 0.204 |
| 32 | Uracil ... Ethyne | 0.199 |
| 33 | Pyridine ... Ethene | 0.220 |
| 34 | Pentane ... Pentane | 0.203 |
| 35 | Neopentane ... Pentane | 0.199 |
| 36 | Neopentane ... Neopentane | 0.193 |
| 37 | Cyclopentane ... Neopentane | 0.200 |
| 38 | Cyclopentane ... Cyclopentane | 0.202 |
| 39 | Benzene ... Cyclopentane | 0.218 |
| 40 | Benzene ... Neopentane | 0.214 |
| 41 | Uracil ... Pentane | 0.208 |
| 42 | Uracil ... Cyclopentane | 0.210 |
| 43 | Uracil ... Neopentane | 0.205 |
| 44 | Ethene ... Pentane | 0.194 |
| 45 | Ethyne ... Pentane | 0.199 |
| 46 | Peptide ... Pentane | 0.201 |
| 47 | Benzene ... Benzene (TS) | 0.214 |
| 48 | Pyridine ... Pyridine (TS) | 0.208 |
| 49 | Benzene ... Pyridine (TS) | 0.210 |
| 50 | Benzene ... Ethyne (CH-pi) | 0.192 |
| 51 | Ethyne ... Ethyne (TS) | 0.136 |
| 52 | Benzene ... AcOH (OH-pi) | 0.191 |
| 53 | Benzene ... AcNH2 (NH-pi) | 0.184 |
| 54 | Benzene ... Water (OH-pi) | 0.174 |
| 55 | Benzene ... MeOH (OH-pi) | 0.198 |
| 56 | Benzene ... MeNH2 (NH-pi) | 0.206 |
| 57 | Benzene ... Peptide (NH-pi) | 0.208 |
| 58 | Pyridine ... Pyridine (CH-N) | 0.177 |
| 59 | Ethyne ... Water (CH-O) | 0.015 |
| 60 | Ethyne ... AcOH (OH-pi) | 0.129 |
| 61 | Pentane ... AcOH | 0.193 |
| 62 | Pentane ... AcNH2 | 0.196 |
| 63 | Benzene ... AcOH | 0.204 |
| 64 | Peptide ... Ethene | 0.182 |
| 65 | Pyridine ... Ethyne | 0.136 |
| 66 | MeNH2 ... Pyridine | 0.202 |

S6. REFERENCES

- ¹Z.-F. Liu and K. Burke, Physical Review A **79**, 064503 (2009).
²M. Seidl, P. Gori-Giorgi, and A. Savin, Physical Review A **75**, 042511 (2007).

³S. Vuckovic, T. J. Irons, A. Savin, A. M. Teale, and P. Gori-Giorgi, *J. Chem. Theory Comput.* **12**, 2598 (2016).

⁴A. Teale, S. Coriani, and T. Helgaker, *The Journal of chemical*

physics **130**, 104111 (2009).

⁵S. Vuckovic, P. Gori-Giorgi, F. Della Sala, and E. Fabiano, *J. Phys. Chem. Lett.* (2018).